

LIBRARY
COPY

STUDY OF A NERNST TYPE GAS TURBINE

by

H. Joseph Myers

and

John G. Polk

Submitted in Partial Fulfillment of the
Requirements for the Degree of

BACHELOR OF SCIENCE

in

CHEMICAL ENGINEERING

from the

MASSACHUSETTS INSTITUTE OF TECHNOLOGY
Cambridge, Massachusetts

June 1953

Signatures of Authors:

H. Joseph Myers
John G. Polk

Signature of Thesis Supervisor:

Harold C. Weber
Harold C. Weber

Signature of Head, Department
of Chemical Engineering

Edwin R. Gilliland

LIBRARY
COPY

STUDY OF A NERNST TYPE GAS TURBINE

by

H. Joseph Myers

and

John G. Polk

Submitted in Partial Fulfillment of the
Requirements for the Degree of

BACHELOR OF SCIENCE

in

CHEMICAL ENGINEERING

from the

MASSACHUSETTS INSTITUTE OF TECHNOLOGY
Cambridge, Massachusetts

June 1953

Signatures of Authors:

Signature redacted

Signature redacted

Signature of Thesis Supervisor:

Signature redacted

Harold C. Weber

Signature of Head, Department
of Chemical Engineering

Edwin R. Gilliland

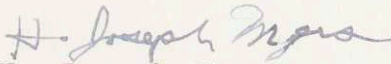
Department of Chemical Engineering
Massachusetts Institute of Technology
Cambridge 39, Massachusetts
May 25, 1953

Professor Earl B. Millard
Secretary of the Faculty
Massachusetts Institute of Technology
Cambridge 39, Massachusetts

Dear Sir:

The thesis entitled "Study of a Nernst Type Gas Turbine" is hereby submitted in partial fulfillment of the requirements for the degree of Bachelor of Science in Chemical Engineering.

Respectfully,


H. Joseph Myers


John G. Polk

Department of Chemical Engineering
Massachusetts Institute of Technology
Cambridge 39, Massachusetts
May 25, 1953

Professor Earl B. Millard
Secretary of the Faculty
Massachusetts Institute of Technology
Cambridge 39, Massachusetts

Dear Sir:

The thesis entitled "Study of a Nernst Type Gas Turbine" is hereby submitted in partial fulfillment of the requirements for the degree of Bachelor of Science in Chemical Engineering.

Respectfully,

Signature redacted

H. Joseph Myers

Signature redacted

John G. Polk

ACKNOWLEDGMENT

We would like to take this opportunity to express our appreciation to Professor Harold C. Weber for the interest he has shown in this thesis and for his constructive criticism and suggestions.

We would also like to thank Messrs. Henry Chasen, Harry Archibald, Allan Merrill, and Schuyler Holbrook for their help in the construction of the combustion chamber and auxiliary parts used in this thesis.

H.J.M.

J.G.P.

TABLE OF CONTENTS

	<u>Page No.</u>
I. SUMMARY	1
II. INTRODUCTION	3
III. PROCEDURE	17
IV. RESULTS	27
V. DISCUSSION OF RESULTS	31
VI. CONCLUSIONS	37
VII. RECOMMENDATIONS	39
VIII. APPENDIX	40
A. Maximum allowable peripheral velocity, Sample Calculation	41
B. Derivation, ideal cycle efficiency . .	41
C. Derivation, maximum allowable pressure ratio	44
D. Derivation, propulsion power	45
E. Derivation, exhaust velocity	46
F. Derivation, propulsion efficiency . . .	46
H. Derivation, nozzle designs	47
I. Results, Sample Calculation	48
J. Calibration Curves	51
K. Original data	53
L. Nomenclature	54
M. Literature citations	57

LOCATION OF TABLES AND FIGURES

<u>Table</u>	<u>Title</u>	<u>Page</u>
I	Stress characteristics of RC-130-B	7
II	Effect of varying the ratio h_o/h on maximum peripheral speeds	7
III	Relation between decisive design charac- teristics and ideal cycle efficiency, propulsion efficiency, power output, etc. . .	16
IV	Summary of experiments	29

<u>Figure</u>	<u>Title</u>	<u>Page</u>
1	Turbine disc, cross section	6
2	Schematic diagram, combustion chamber	6
3	Nozzle characteristics	13
4	Converging-diverging nozzle	13
5	Static test combustion chamber	18
6	System flow sheet	21
7	Reaction wheel gas turbine	22
A	Thermodynamic diagram	41

I. SUMMARY

The purpose of this thesis was to construct and operate a combustion chamber compatible in design with jet combustion chambers built into the periphery of a proposed Nernst-type reaction gas turbine. This type of turbine could be used commercially where a compact, cheap, high-speed power plant is desirable. The proposed turbine would consist of a six inch diameter metallic disc with two or more jets built at the periphery (see Figure 7).

It was found that although this power plant could operate at higher temperatures than ordinary gas turbines, this thermodynamic advantage was offset by the maximum peripheral speed allowable in known metallic alloys such as RC-130-B before failure occurs.

Other disadvantages are the low efficiencies resulting from this type of power plant. In the Nernst-type chamber, compression, combustion, and expansion must be conducted in one stage and in a small volume. In the regular gas turbines these steps are carried out in separate stages enabling the careful control of each step to assure the attainment of the optimum thermodynamic conditions.

Investigations were carried out by using a static test chamber of dimensions similar to those that would be used in the actual turbine (see Figures 5 and 7). Several operations

were carried out at various chamber pressures. The operating conditions of the best of these runs are listed below:

Pressure at chamber inlet	60 psig.
Internal efficiency	8.7 per cent
Internal power	5.7 HP./jet
Ideal cycle efficiency	37.1 per cent
Combustion rate	28.8 million $\frac{\text{BTU}}{\text{hr.}-\text{ft.}^3}$
$\frac{\text{Oxygen}}{\text{Propane}}$ ratio, (weight basis)	1.76
Secondary air flow at 1 atm.	9.35 ft. ³ /min.
Primary air flow at 1 atm.	1.40 ft. ³ /min.

Optimum operating conditions were not achieved due to limitations in the volumetric capacities of the air streams. Higher power output and efficiencies may be obtained if the maximum capacities of the primary and secondary air streams are increased. Higher chamber pressures will also result in better efficiencies and higher power output.

It is recommended that further investigations be made to determine the optimum operating conditions at one chamber pressure in the neighborhood of 60 psig. before design and construction of the actual turbine be attempted.

II. INTRODUCTION

The purpose of this thesis was to build and operate a jet combustion chamber compatible in design with jet combustion chambers to be used in a proposed Nernst-type reaction gas turbine. This type of turbine would fit applications where a compact, high-speed power plant is desirable.

At the time of previous investigations (1949), metallurgical difficulties restricted the operating speed of the proposed turbine to 48,900 (with no safety factor). In this range the efficiencies and power output of the turbine were found to be quite low (an efficiency of 3.8 o/o and a power output of 0.32 HP/jet were the maximum found) (6).

However, with the rapid progress of the development of titanium alloys, the operating range of the turbine speed may be greatly increased. For this reason this thesis was undertaken to study the power output and efficiency of the proposed chamber in the higher pressure range afforded by the higher velocities. The pressure range in these studies was above that necessary to induce sonic velocities in the exhaust gases. Therefore, it was necessary that the test chamber be equipped with a converging-diverging nozzle to minimize shock waves.

The proposed turbine would consist of two or more combustion chambers rotating about a common axis. These chambers behave essentially as ram jets, receiving fuel through the shaft about which they rotate. The air for combustion could be introduced either through the shaft or as ram air at the periphery of the turbine. In either case, by virtue of a high peripheral speed, the gases will enter the chamber at a reasonably high pressure. The air would mix with and oxidize the fuel, and expand through a converging-diverging nozzle finally leaving the turbine at super-sonic speeds (relative to the nozzle) (6).

The exhaust gases, rejected at a substantial absolute velocity, would flow away from the turbine, creating a surge which would cause fresh air to replace it and provide for continuous combustion. The surge of air past the turbine walls would tend to cool the walls of the jets simultaneously preheating the air and hence permit a high nozzle inlet temperature (the temperature reached after combustion and immediately prior to expansion through the nozzle). A high nozzle inlet temperature permits a high average temperature of heat reception and therefore a high Carnot efficiency.

The need for a compressor would be eliminated in this power plant. The ram or the centrifugal forces would supply the necessary compression for the air and fuel. A

consequence of this would probably be a saving in power losses and a further increase of efficiency over that obtainable with current gas turbines.

A solid cylindrical disc, tapering toward the rim (Figure 1) is known to allow greater peripheral speeds before failure than an untapered one. This can be expressed quantitatively by the equation (6):

$$\frac{\sigma}{\gamma} = \frac{\omega^2 x^2}{2g \ln(h_0/h)} \quad (1)$$

where h , is the thickness at radius x (inches); h_0 , is the thickness at the axis (inches); ω , is the maximum allowable angular velocity (radians per second); γ , the density of the metal (pounds per cubic inch); σ , the maximum allowable stress (psi.). From this it can be seen that an increase in the maximum allowable angular velocity is favored by a metal of high tensile strength and low density, and by an increase in the ratio h_0/h .

A survey of existing materials showed that metals of low density usually have a low melting point and are therefore not suitable for turbine construction (4). A notable exception is titanium. At the suggestion of Professor H. C. Weber, the possibility of constructing the turbine of a suitable titanium alloy was investigated. It was found that a titanium-base alloy, RC-130-B, is now available

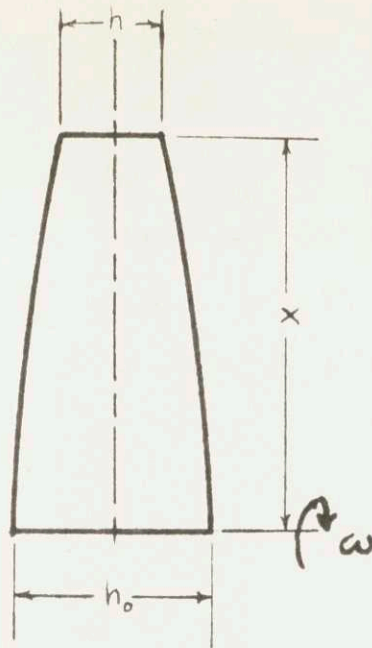


Figure 1

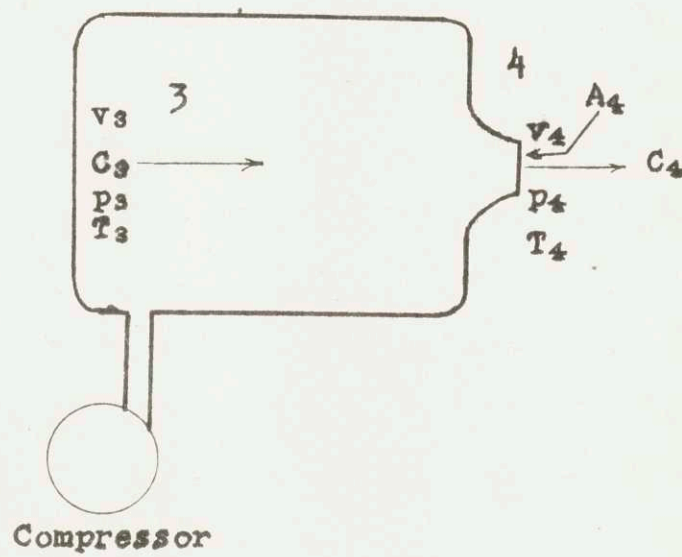


Figure 2

which has the following properties (5):

TABLE I

<u>Temperature, °F</u>	<u>68</u>	<u>200</u>	<u>400</u>	<u>600</u>	<u>700</u>	<u>800</u>
Tensile Yield Strength x 10 ³ , psi.	130	122	107	92	86	76
Composition	4% Aluminum, 4% Magnesium, 92% Titanium					
Density, lbs./in ³	0.165					

These properties compare favorably with heavier metal alloys such as the Chromium-Nickel-Cobalt alloy, K-42-B (4). K-42-B has a high tensile strength (91,200 psi.) which is relatively independent of temperatures below 1200°F: it has a density of 0.33 pounds/inch³.

An increase of the ratio of h_o/h will also result in a larger allowable angular velocity. However, Table II indicates that for ratios of h_o/h greater than three, the relatively small increases in the natural log of h_o/h probably do not justify the added material expense of constructing a wheel with a width ratio greater than three or possibly four.

TABLE II

<u>h_o/h</u>	<u>1</u>	<u>2</u>	<u>3</u>	<u>4</u>	<u>5</u>	<u>6</u>	<u>7</u>
$\ln(h_o/h)$	0	0.69	1.10	1.39	1.61	1.80	1.95

Thus, for example, a wheel constructed of RC-130-B at 700°F with \underline{x} equal to three inches, h_o/h equal to three and a factor of safety equal to 1.2; a maximum rim speed of 1610 ft./sec. is obtained. If one now uses a h_o/h equal to four the new maximum rim speed becomes 1810 ft./sec. (see Appendix A).

For an ideal gas turbine (ideal compressor, combustion chamber, and nozzle) using air as a working fluid, the thermodynamic efficiency is given by the relation:

$$\eta_T = 1 - \left(\frac{1}{r}\right)^{\frac{k-1}{k}} \quad (2)$$

(see Appendix B) where $\underline{\eta}_T$ is the ideal efficiency for the non-regenerative cycle; \underline{r} , the ratio of the pressure inside the combustion chamber to the exhaust pressure; and \underline{k} the ratio of the specific heat, C_p/C_v . Equation (2) is independent of temperature. This does not contradict the fact that the higher the temperature of heat reception, average sink temperature (rejection temperature) remaining constant, the higher the Carnot efficiency; for a consideration of the derivation of equation (2) will show that an increase in the ratio of the chamber temperature to the sink temperature increases the pressure ratio, \underline{r} . Thus, equation (2) is consistent with the temperature trends of Carnot efficiencies.

Since the thermodynamic efficiency of the turbine depends solely on the pressure ratio, r , it is necessary to find the maximum r obtainable for a wheel that is rotating at its maximum peripheral speed. Consider then, the turbine rotating at v_{\max} , and a unit mass of exhaust gas leaving the turbine at negligible absolute velocity. Then an energy balance gives:

$$T_3 = T_4 + \frac{v^2}{2gC_p J} \quad (3)$$

If one then defines the mach number, M , as the velocity of the turbine gas divided by the acoustic velocity of the gas (10).

$$M = \frac{v}{\sqrt{kg RT_4}} \quad (4)$$

Substitution of equation (4) into equation (3) and rearrangement gives (see Appendix C):

$$r = \frac{p_3}{p_4} = \frac{p_2}{p_1} = \left(1 + \frac{(k-1)}{2} M^2\right)^{\frac{k}{k-1}} \quad (5)$$

It is obvious that a high propulsion power as well as a high thermodynamic efficiency is desirable. The propulsion power can be considered as the energy supplied by the turbine which is available as absolute kinetic energy of the gases and the torque power (3):

$$P = \frac{G}{2g} (C - v)^2 + (F_d + F_n)v \quad (6)$$

$$P = \frac{G}{2g} (C^2 - v^2) = \frac{G}{2g} v^2 \left(\frac{1}{\theta_2} - 1 \right) \quad (7)$$

where \underline{P} is the propulsion power; \underline{G} , the weight rate of flow of the exhaust gases; and \underline{C} , the velocity of the exhaust gases relative to the turbine nozzle (see Appendix D).

Equation (7) shows that P can be increased by increasing \underline{G} or \underline{C} , or by decreasing \underline{v} . \underline{G} is limited by the size and design of the combustion chamber; a decrease in \underline{v} results in a lower pressure ratio, \underline{r} , and therefore a lower thermodynamic efficiency. \underline{C} can be increased by raising the nozzle inlet temperature. This can be accomplished by pre-heating the fuel and secondary-air ducts. (see Appendix E).

$$C = \frac{\sqrt{2g k R T_3 \eta_T}}{\sqrt{m (k - 1)}} \quad (8)$$

An increase in \underline{C} does not effect the ideal thermodynamic efficiency. However, it must be remembered that (the ideal thermodynamic efficiency) can only be approached when the absolute velocity of the exhaust gases is negligible; that is, when $\underline{C} = \underline{v}$. For this condition, the propulsion power, \underline{P} , equals zero as can be seen by substituting $C = v$ into equation (7). An increase in \underline{C} also has the further drawback of decreasing the propulsion efficiency, (fraction of

propulsion power available as torque power).

$$\eta_p = \frac{(F_d + n)v}{(F_d + n)v + \frac{G}{2g}(C - v)} = \frac{2v/C}{1 + v/C} = \frac{2\theta}{1 + \theta} \quad (9)$$

(see Appendix F)

Further, the torque power,

$$\begin{aligned} P_{d+n} &= F_d + n v = P \eta_p \\ &= \frac{G}{2g} v^2 \left(\frac{1}{\theta^2} - 1 \right) \frac{2\theta}{1 + \theta} \\ &= \frac{G}{g} v^2 \left(\frac{1 - \theta}{\theta} \right) \end{aligned} \quad (10)$$

and,

$$\frac{\partial P_{d+n}}{\partial \theta} = - \frac{Gv^2}{g\theta^2} \quad (11)$$

which is always negative. Since θ equals v/C , and increase in \underline{C} will always result in an increase in P_{d+n} . Therefore, an increase in the inlet nozzle temperature results in an increase of \underline{C} , \underline{P} , and P_{d+n} , but does so at the expense of propulsion efficiency.

It can be shown that, if an ideal gas flows through a hundred percent converging nozzle under steady-state conditions with no heat added or mechanical work removed (see Figure 2), the exit velocity, C_4 , is (10):

$$C_4 = \sqrt{2g \frac{k}{k-1} RT_3 \left[1 - \left(\frac{p_4}{p_3} \right)^{\frac{k-1}{k}} \right]} + C_3 \quad (12)$$

The weight rate of flow is:

$$G = C_4 A_4 \rho_4 = C_3 A_3 \rho_3 \quad (13)$$

where

$$(\rho_4)^2 = \left(\frac{1}{v_4} \right)^2 = \frac{1}{v_3^2} \left(\frac{p_4}{p_3} \right)^{\frac{2}{k}} \quad (14)$$

for adiabatic expansion. Substitution of equations (13) and (14) into equation (12) and making the assumption that C_3 is negligible gives:

$$G = A_4 \sqrt{\frac{2gk}{k-1} \frac{p_3^2}{RT_3} \left[\left(\frac{p_4}{p_3} \right)^{\frac{2}{k}} - \left(\frac{p_4}{p_3} \right)^{\frac{k+1}{k}} \right]} \quad (15)$$

A consideration of equation (13) will show that there are two conditions for which the weight rate of flow, G , is zero. One corresponds to zero pressure drop ($C_4 = \text{zero}$, and $p_3 = p_4$); the other occurs when the gas is expanded into a vacuum ($\rho_4 = \text{zero}$, and $p_4 = \text{zero}$). Thus it follows (see Figure 3) that between these two limits of the expansion ratio at least one maximum value of G must exist. Previous investigators have shown that only one such maximum exists. This can be obtained by differentiating equation (15) (with respect to $\left(\frac{1}{r} \right)$ and setting the result equal to zero):

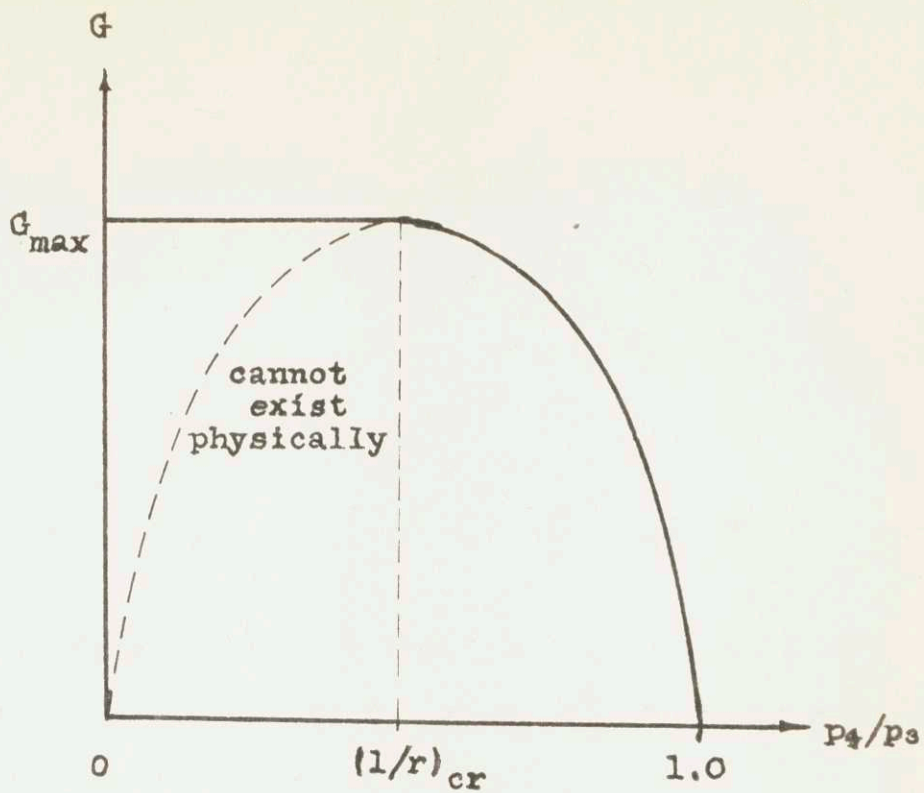


Figure 3

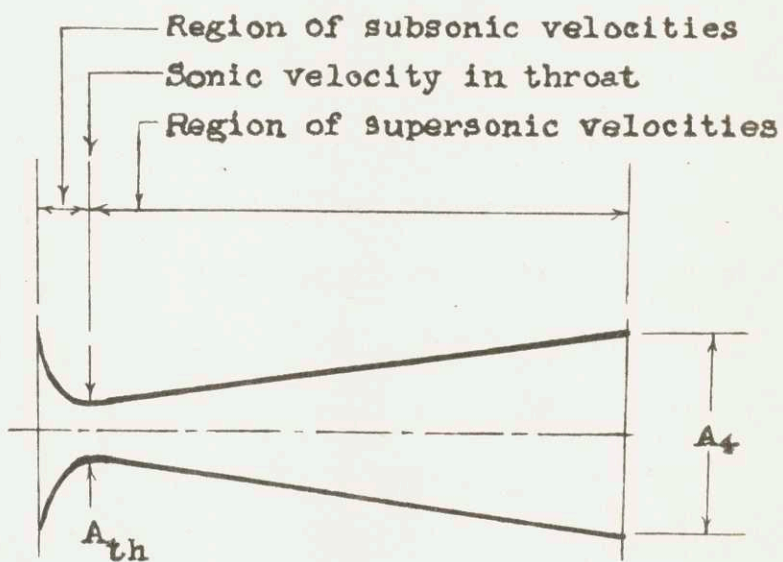


Figure 4

$$\frac{d \left[\left(\frac{p_4}{p_3} \right)^{\frac{2}{k}} - \left(\frac{p_4}{p_3} \right)^{\frac{k+1}{k}} \right]}{d (p_4/p_3)} = 0 \quad (16)$$

The result of the differentiation gives the critical pressure ratio corresponding to the maximum \underline{G} :

$$\left(\frac{p_4}{p_3} \right)_{cr.} = \frac{1}{r_{cr.}} = \left(\frac{2}{k+1} \right)^{\frac{k}{k-1}} \quad (17)$$

Substitution of equation (17) into equation (12) and again neglecting the chamber gas velocity, C_3 , gives the critical exhaust speed corresponding to G_{max} :

$$C_4 = (gkRT_4)^{\frac{1}{2}} \quad (18)$$

which is identical with the local acoustic velocity. Further, substitution of equation (17) into (15) gives:

$$G_{max} = 3.89 \frac{A_4 p_3}{\sqrt{R T_3}} \quad \text{for } k = 1.4 \quad \text{(air)} \quad (19)$$

If one now uses \underline{k} equal to 1.4 in equation (17) the critical pressure ratio for air becomes $p_3/p_4 = 1.89$. Thus when the pressure ratio, \underline{r} , ($r = p_3/p_4$) is 1.89, the exhaust gases leave the nozzle at the acoustic velocity. Previous investigations have shown that, if \underline{r} is increased above this critical value, the additional available energy is not transformed into kinetic energy, but is used up in frictional heat and noise after the gas jet emerges from the converging nozzle.

De Laval showed that a correctly designed converging-diverging nozzle will convert all of the expansion energy into kinetic energy for pressure ratios larger than 1.89. Such a nozzle requires that the critical pressure ratio exists at the throat, and that the area ratio of the diverging section be such that:

$$A_4 \psi_4 = A_t \psi_{\max} \quad (20)$$

where

$$\psi = \sqrt{\frac{k}{k-1}} \sqrt{\frac{z}{1+z}} (r)^{\frac{1}{k}}$$

$$z = (r)^{\frac{k-1}{k}} - 1$$

$$\text{and } \psi_{\max} = \psi_{\max.} \text{ at } r = r_{\text{critical}}$$

This results in the following nozzle-design equation:

$$\frac{A_t}{A_4} = \left(\frac{k-1}{2}\right)^{\frac{1}{k-1}} \sqrt{\frac{k+1}{k-1} \left[\left(\frac{p_4}{p_3}\right)^{\frac{2}{k}} - \left(\frac{p_4}{p_3}\right)^{\frac{k+1}{k}} \right]} \quad (21)$$

(see Figure 4). Appendix H gives a more detailed development of the equations in the above section on nozzles.

TABLE III

$\frac{h_o}{h}$	$\ln \frac{h_o}{h}$	v_{max}	M	r_{max}	η_T	$\frac{C}{\text{at } 2000^\circ R}$	θ	η_p	$\eta_T \cdot \eta_p$	G_s lbs./sec.	P_{n+d} (HP)
3	1.1	1610	1.44	3.35	.292	2380	.667	.808	.236	.00216	1.94
4	1.39	1810	1.62	4.39	.345	2480	.730	.850	.293	.00318	2.64
5	1.61	1950	1.745	5.28	.378	2595	.752	.858	.324	.00382	3.50

Table 3 shows the relation between the decisive design characteristics and theoretical net efficiency ($\eta_T \times \eta_p$), theoretical power output, and weight rate of flow.

III. PROCEDURE

The usual technique used to study the performance of rockets and ram jets is that of the static test. The scope of this thesis is limited to the construction of a combustion chamber compatible with a turbine design proposed by G. A. Sofer, and the study of the net efficiency and power output of the turbine indirectly by means of a static test (6).

Experimental Objectives

The objectives of the experimental work were:

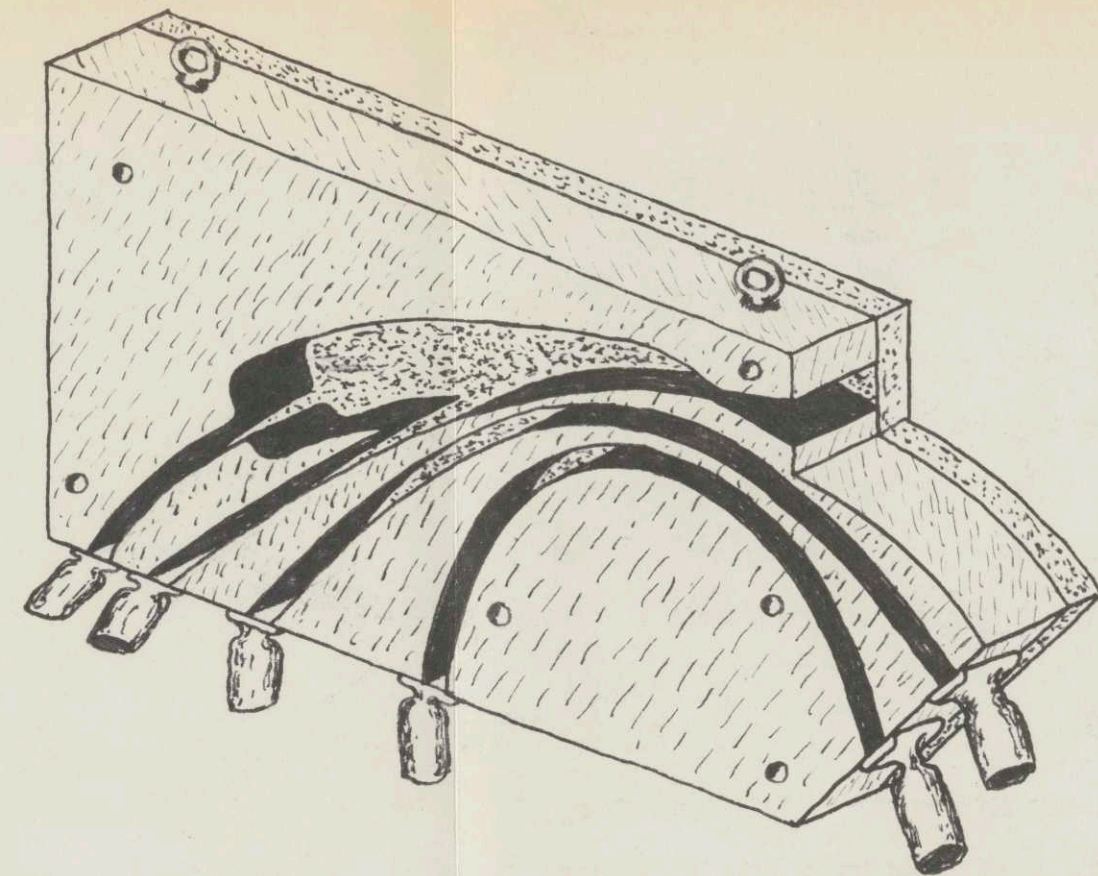
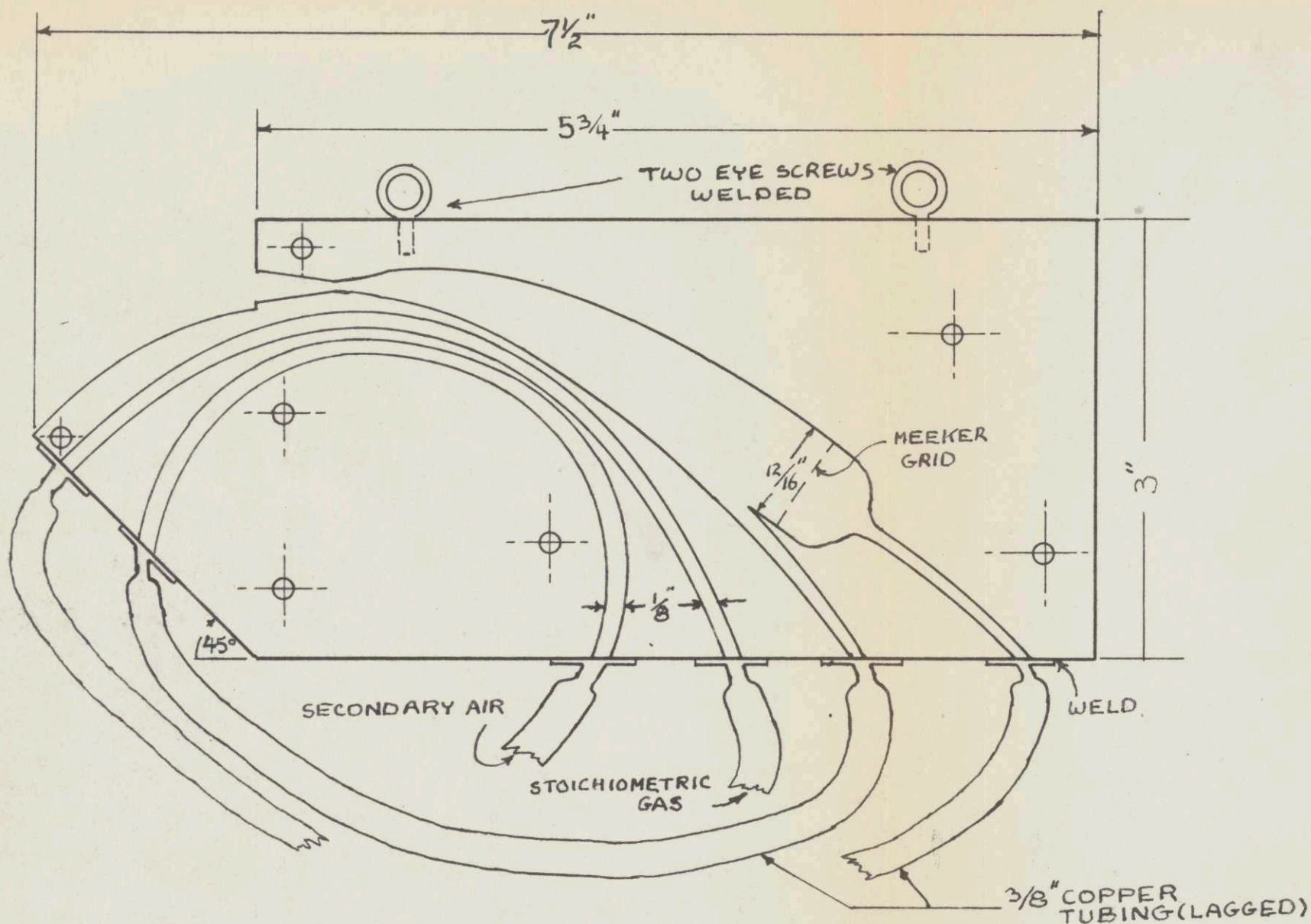
(a) A study of the combustion of propane in a chamber of such size and shape as to approximate the combustion chamber of a Nernst-type turbine, with the aim of operating at the highest possible velocity before "blow out" (i.e., the flame leaves the chamber).

(b) The determination of net, or overall, efficiency and power output at various chamber pressures.

(c) An estimation of the deviation of the actual internal efficiency with the ideal cycle efficiency.

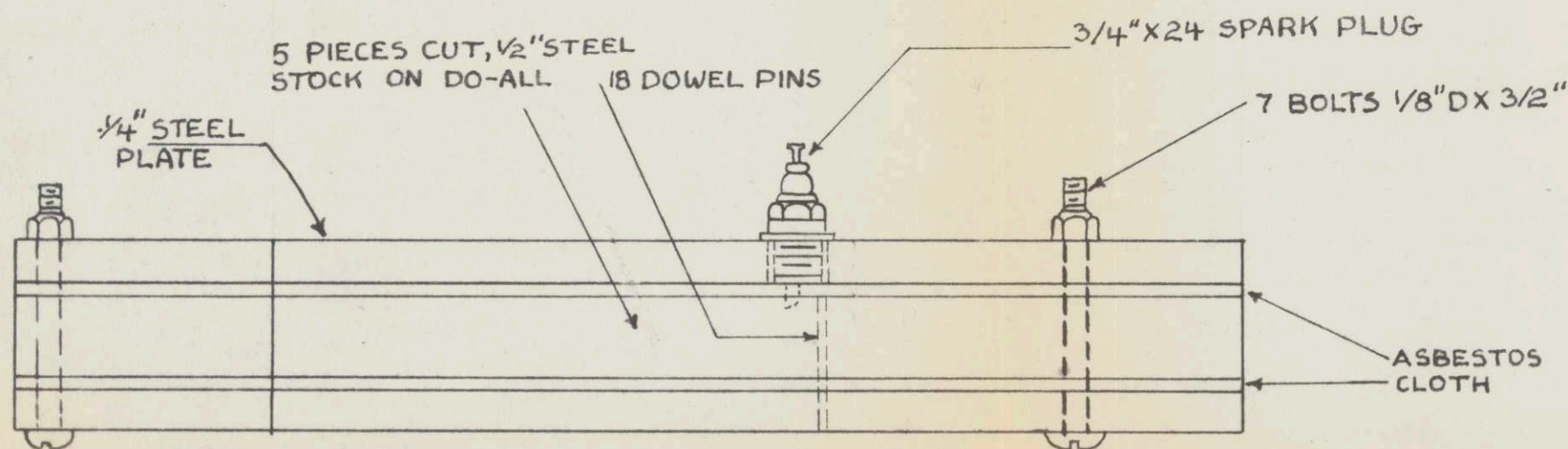
Apparatus

The combustion chamber (hereafter referred to as "the unit") used in the static tests is described in Figure 5



STATIC TEST COMBUSTION CHAMBER

FIGURE 5



under the title, "Static Test Combustion Chamber." Cold rolled mild steel was used for the construction of the unit; all pieces were cut out on a Do-All. Copper tubing was used to conduct gases into the unit. The copper tubing used for the pre-heat was lagged with asbestos. The central half-inch pieces were dowelled to the bottom cover plate. An asbestos cloth gasket was secured between the central section and the bottom cover plate to insure that the unit was air tight. The top cover plate was secured to the rest of the unit by seven bolts, $1/8$ " DX $1\ 1/2$ ". Here also, an asbestos cloth gasket was placed between central section and top cover plate.

Propane and air were metered separately into a premixer from which they flowed as a stoichiometric mixture into the inlet of the test unit. Secondary air was metered directly into the unit's secondary air inlet from the Institute's high pressure line. Three orifice meters were used to measure the rate of flow of the gases. The manometers were made of tygon tubing to eliminate the hazard of glass breakage at high pressures. The manometer fluid was water. The downstream pressure for the line carrying the stoichiometric mixture of propane and air was measured with a gauge located on the premix tank. The downstream pressure of the secondary air line was measured by a gauge located next to the secondary air orifice meter.

All lines were constructed of 1/4" copper tubing except where flexibility was necessary. In those sections 1/4" tygon tubing was used. Figure(6) is a schematic diagram of the testing system used.

The premixer was a high pressure steel vessel (to give protection in case of explosion) and was fitted with a 150-mesh screen on the outlet to prevent a flashback of the explosive propane-air mixture.

A model airplane spark plug was installed in the top cover plate to initiate combustion in the chamber. A Tesla coil which generates high frequency current was used to fire the spark plug. The Tesla coil has the property of developing a spark when the wire extending from the head of the coil is brought near a metallic surface. It is not necessary that the metallic surface be grounded. The spark is of the same nature as that which takes place upon transfer of high voltage static charge from one conductor to another. The larger the capacity of the conductor, the longer and brighter the spark. By touching the metallic head of the spark plug with the Tesla coil wire, the central electrode is made part of the coil and a spark develops between this and the outer electrode.

A Meeker grid was installed in the upstream section of the combustion chamber to aid flame propagation.

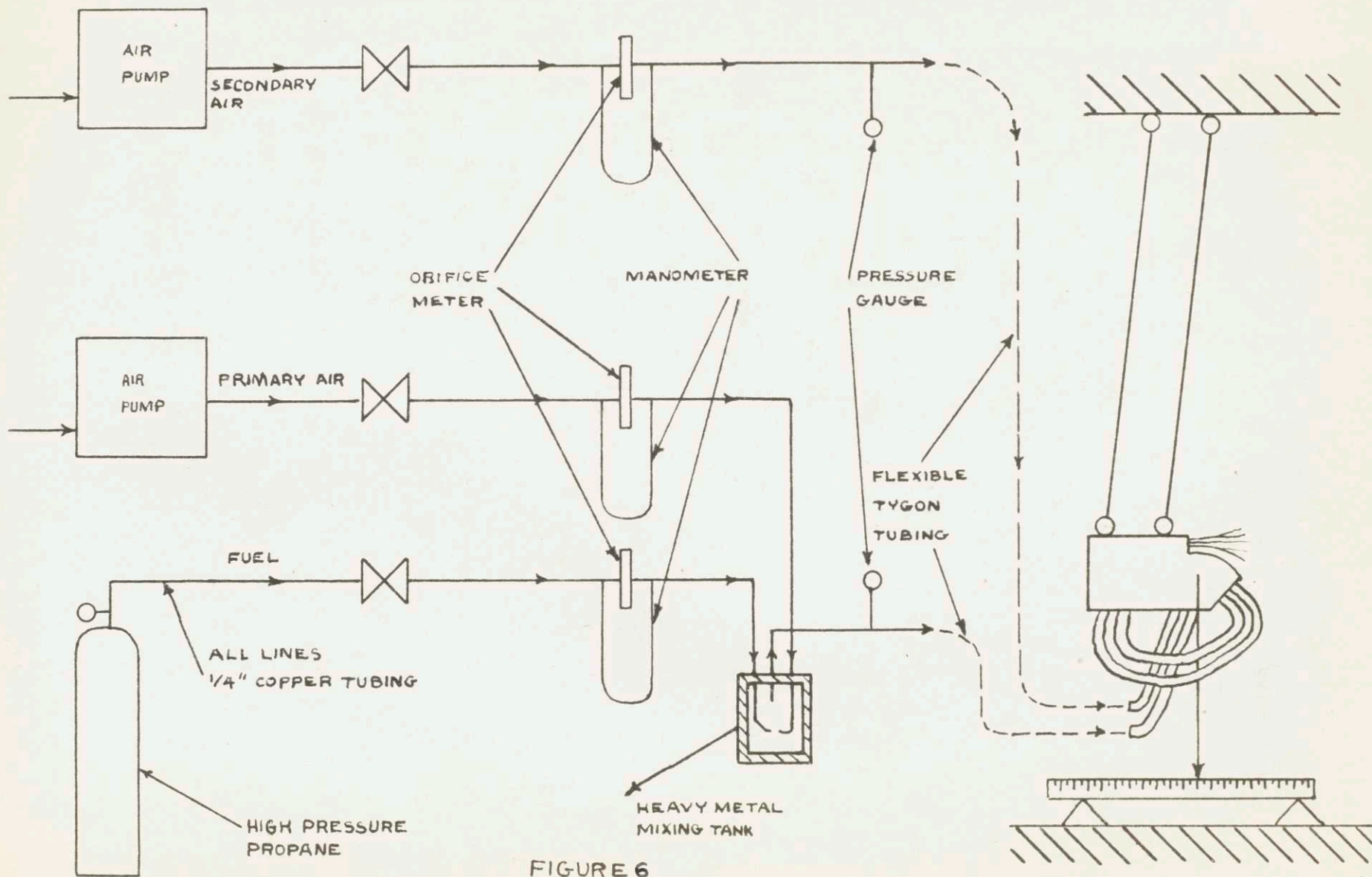
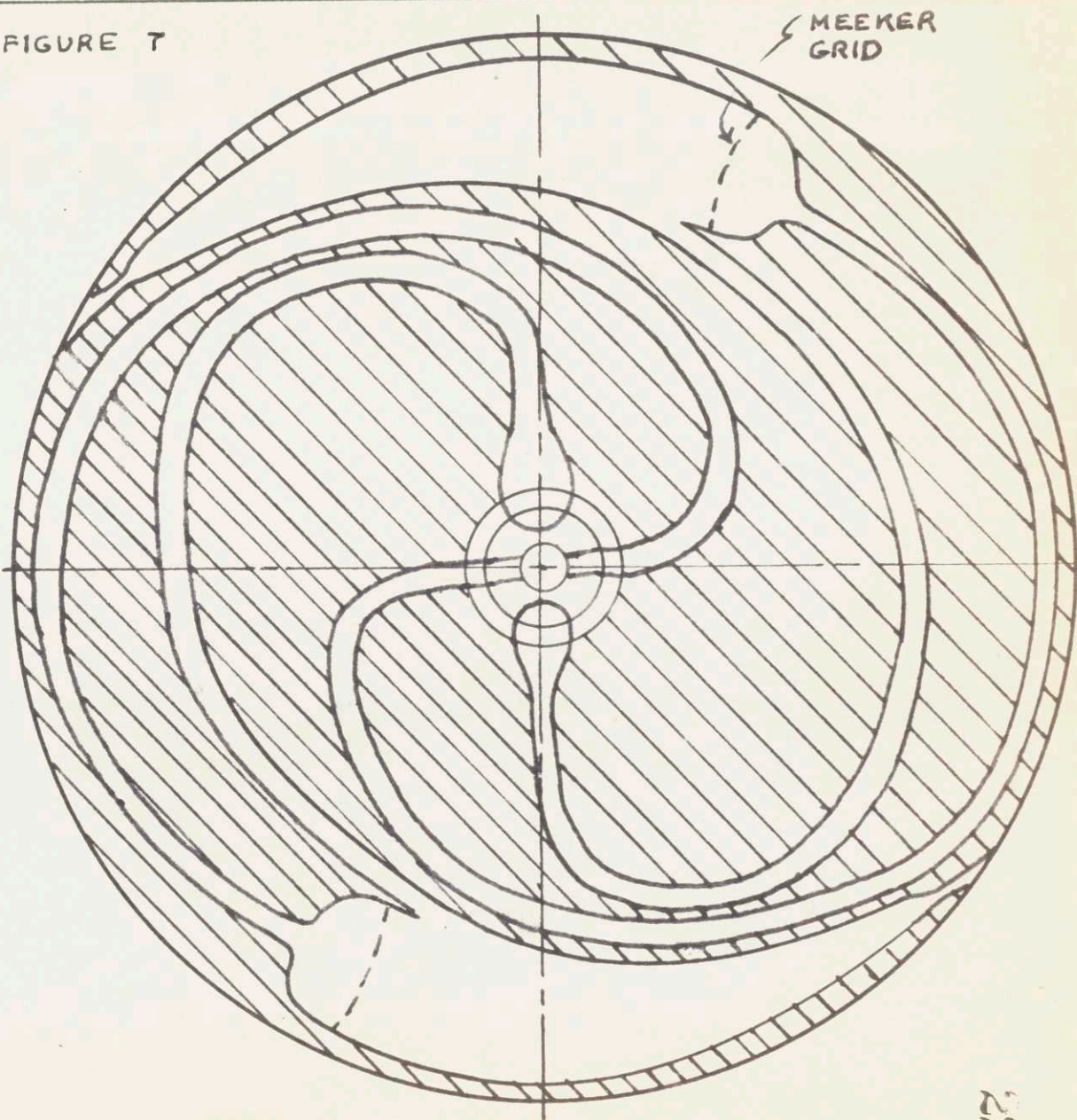
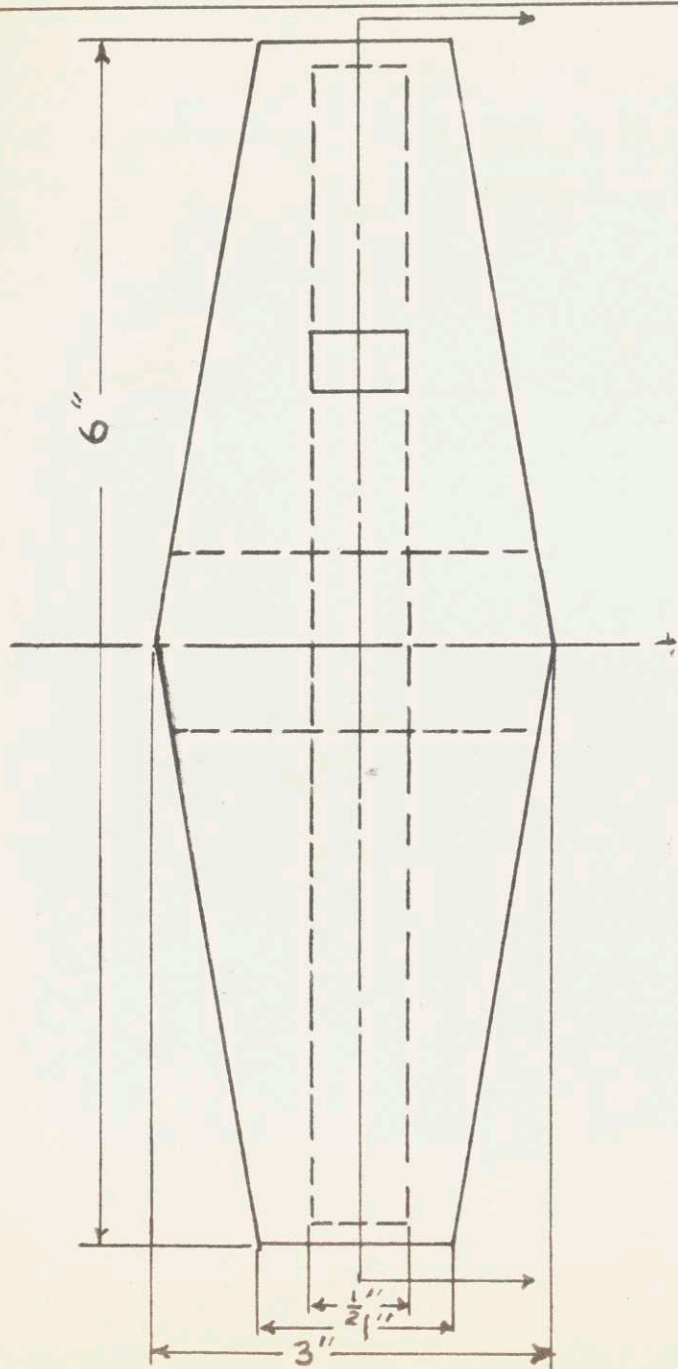


FIGURE 6

SYSTEM FLOW SHEET

FIGURE T



REACTION WHEEL GAS TURBINE

The unit was hung in a horizontal position by attaching steel wire leads from an overhead horizontal bar to two eye screws welded onto the top of the central section of the unit. A thin steel pointer was brazed to the cover plate in a vertical position. A meter stick was fastened in a horizontal position directly below the suspended test unit. The gases burning in the test unit expanded the secondary air and the resulting thrust was indicated by the deflection of the unit from its natural suspended position. Since the deflections in the test runs were small, the thrust was directly proportional to the measured deflection of the pointer on the meter stick; i.e., thrust was directly proportional to net deflection (deflection during "hot" part of the run (fuel burning) minus deflection during "cold" part of the run (fuel not ignited)).

Experimental Methods

The calibration of the orifice meters at various line pressures was accomplished by using a standard dry-test gas meter and stopwatch.

Power output was determined by the static test method. As mentioned previously the unit was suspended on two wires. The thrust of the exhaust gases was determined from the deflection of the wire from the vertical. Two runs were made at each desired pressure; one was a "hot run;" the

other a "cold run." This enabled the computation of the energy output due to the combustion alone. Methods of calculation are outlined in Appendix "I" under the heading, "Calculations."

Experiments

1. Testing System for Leaks

The entire system of gas lines and flow meters was tested for leaks in the following manner:

(a) Screw clamps were used to close off the tygon tubing near the test unit inlets.

(b) Air from the Institute's high pressure line was bled into the system and the valve was adjusted so that a constant pressure was maintained.

(c) All joints were bathed in a soap and water solution which disclosed leaks by the formation of soap bubbles.

Leaks were eliminated by further tightening of fittings in some cases and the use of red glyptal binder in others.

2. Calibration of Orifice Meters

Air from the Institute's high pressure line was passed through each orifice meter and then through a dry test meter. The downstream pressure and the manometer reading was recorded. The dry-test meter measured the volumetric through-put (at atmospheric conditions) over a given period

of time. The period elapsed for each run was recorded by a stopwatch. This enabled one to determine the gas rate of flow under atmospheric conditions. By assuming that the ideal gas laws were valid in the temperature and pressure ranges being studied, simple calculations enabled one to convert the flow rate data at atmospheric conditions to the relevant flow rates at line conditions. Appendix "I" gives such a sample calculation.

The flow rates and pressures could be adjusted by manipulating respectively a screw clamp on the downstream line and a valve on the upstream line. In this way a good range of rates were obtained for each meter at various pressures. The temperature and barometric pressure were recorded for each run.

3. Measuring Dimensions of the Unit

4. Experiment A

This consisted of a trial operation to gain familiarity in controlling the gas rates of flow. The primary air was allowed to flow into the chamber and the spark from the Tesla coil turned on. The propane was then turned on and the flow increased until the flame became stable. Different mixtures of propane and primary air were tried and notice was taken of the manometer readings at which the flame burned with the most stability. These readings were used successfully in later starting attempts.

5. Experiment B.

The purpose of this experiment was to obtain data from which the power output and efficiency of the unit could be calculated. Flow rates and deflections were measured at different chamber pressures and with varying ratios of (a) propane-to-primary air and (b) secondary air-to-fuel mixture.

The propane-primary air mixture was first allowed to stabilize as described in Experiment B. The chamber was allowed to warm up before an attempt was made to use the secondary air.

Flow rates, pressures and deflections were recorded for use in calculations (see Results).

Each combination was termed a "run" and for each run the propane was turned off and the "cold" gases were left running. The deflection from the cold part of the run was recorded as was the approximate exit gas temperature. The flow rate of the propane was about three hundredth of the total gas flow, so that the difference in deflection for the hot and cold parts of the run was essentially entirely due to combustion. Five such runs were made.

IV. RESULTS

Important experimental results are tabulated in the same order as the experiments were discussed in the preceding section.

1. Calibration of Orifice Meters

Three sets of calibration curves constructed from the calibration data are found in Appendix "J". Experimental points are not plotted. No way was found to determine the accuracy of the dry-test meter itself. The accuracy of reading the dry-test meter decreased as volumetric flow rate increased. It is estimated that the greatest errors (at high flow rates) would approximate two per cent. This estimate is based on the maximum percentage error in rate figures corresponding to a time reading error of one second.

2. Dimensions of the Unit

Width of chamber at grid	12/16 inch
Depth of chamber	1/2 inch
Area of nozzle at the throat, A_t	0.000208 ft. ²
Area of nozzle at the outlet, A_4	0.000230 ft. ²
Weight of unit including copper tubing and lagging	6.25 lbs.
Chamber volume	0.000503 ft. ³

3. Miscellaneous Preliminary Measurements

(a) Maximum pressure developed by the Nash Hytor compressor (primary air pump) was 26 psig.

(b) Maximum pressure developed in the Institute high pressure air line was 60 psig.

(c) Maximum capacity of air lines:

Secondary air stream 7.90

Primary air stream 1.65

(d) Maximum flow available in air lines during runs:

Secondary air stream 9.35

Primary air stream 1.65

4. Experiment B

Table IV summarizes the results obtained in this section. These results are discussed in the next section. A sample calculation is given in Appendix "I".

TABLE IV

Summary of Experiments

<u>Runs</u>	<u>Chamber Pressure psig.</u>	<u>Fuel, Volumetric Rate ft.³/min. at 1 atm.</u>	<u>Primary Air Volumetric Rate ft.³/min. at 1 atm.</u>	<u>Secondary Air Volumetric Rate ft.³/min. at 1 atm.</u>	<u>O₂/propane Wt. basis*</u>	<u>exhaust velocity relative to nozzle C_n ft./sec.</u>
1	9	.07	1.47	2.0	4.95	507
2	14	.05	1.42	2.9	6.68	472
3	34	.06	1.25	5.5	4.90	695
4	50	0.14	1.65	8.1	2.77	703
5	60	0.19	1.40	9.35	1.76	810

* Stoichiometric ratio is 3.64 (assuming complete combustion to CO₂).

TABLE IV (Cont'd)

Summary of Experiments

<u>Runs</u>	<u>theoretical nozzle velocity v ft./sec.</u>	<u>η_p per cent</u>	<u>η per cent</u>	<u>η_T per cent</u>	<u>overall $\eta \times \eta_p$ per cent</u>	<u>Net Power Output HP.</u>	<u>Combustion Rate $\times 10^{-6}$ BTU hr.-ft.³</u>
1	956	81	0.6	12.7	0.5	0.14	0.71
2	1150	77.2	4.8	18.2	3.8	0.83	4.2
3	1597	78	22.3	29.4	17.4	4.61	23.4
4	1813	77.3	7.0	34.4	5.4	3.26	16.5
5	1920	77.6	8.7	37.1	6.8	5.70	28.8

V. DISCUSSION OF RESULTS

Orifice Meter Calibrations

It was pointed out in the RESULTS section that there was no estimate made regarding the error intrinsic to the dry-test meter itself. The largest estimated error incurred in reading the dry-test meter would be approximately two per cent. In addition, errors were probably incurred in drawing the best curves through the plotted experimental points. Most of these points lay on the curves drawn, but some were absurdly off and hence were disregarded. It is estimated that when one adds to the errors mentioned above the additional errors incurred in interpolating between given constant pressure curves, the total error should lie between ten and fifteen per cent.

Chamber Dimensions

Errors incurred in measuring the chamber dimensions were probably less than one per cent. The unit weight was determined with an accuracy of approximately 1.6 per cent.

Originally, the area ratio, A_t/A_4 , was designed for a converging-diverging nozzle appropriate for a chamber pressure of 25 psig. (see equation 21). However, due to difficulties in dowelling the central pieces to the bottom cover plate, the desired area ratio was not obtained. Substitution of the

actual values of A_t and A_4 into equation 21 showed that the actual nozzle would work best with a chamber pressure of approximately 15 psig.

The use of the phrase "chamber pressure" should be clarified. As used in this thesis, chamber pressure actually refers to the highest line pressure. The actual chamber pressure is less than the highest line pressure since there will be a pressure drop across the Meeker grid. This pressure drop may be as high as three psig. (6). Thus, a nozzle design for a chamber pressure of 15 psig. is actually a nozzle design for a maximum line pressure of between 15 and 18 psig.

In any case, since none of the runs were made at the nozzle design pressure, it is to be expected that some energy was lost in the form of shock waves.

Experiments A and B

The main objectives of this thesis were to determine the unit's maximum power output at higher pressures and the efficiency of the unit as a power plant.

Five runs were made with chamber pressures ranging from 9 to 60 psig. It is estimated that the accuracy of the measurements were only ten to twenty per cent. This estimate includes intrinsic errors such as those incurred by ignoring the pressure drop across the Meeker grid, reading errors and calculation errors. With such a large estimated percentage error, more

emphasis should be placed on the trends indicated by the different runs than the absolute figures calculated.

The important trends noted were as follows:

- (a) The internal efficiency increases with an increase in chamber pressure (as predicted by equation 2).
- (b) Power output increased with increased chamber pressure.
- (c) The maximum entrance velocity increases with increased chamber pressure.

Due to lack of time, no data was taken to evaluate the completeness of combustion at the various run conditions. However, it was noted that the internal efficiency does not increase at a rate proportional to the increase in the theoretical ideal cycle efficiency with increased chamber pressure. That is, the ratio of internal efficiency to ideal cycle efficiency decreases with an increase in chamber pressure (and consequently higher amount of secondary air). One possible explanation of this trend is that the secondary air tends to quench the burning gases before combustion is complete. That the length of the flame was shortened perceptibly as the secondary air flow was increased during a run, seems to substantiate this postulation. However, no emphasis should be laid on this postulation until it is verified or disproved by experimental tests on the completeness of combustion.

The overall efficiencies in these experiments, as in previous work (6), were found to be low. This is not surprising when compared with current efficiencies associated with existing jet power plants.

A great deal of confusion may arise in regard to the term efficiency. In this work there are four efficiencies of importance:

- (1) The ideal-cycle efficiency as defined by equation 2.
- (2) The internal or actual cycle efficiency which is equivalent to the work output, energy input ratio.
- (3) The propulsion efficiency which indicates the amount of energy lost due to the fact that the exhaust gases are not leaving the nozzle at zero relative velocity.
- (4) The overall efficiency which is defined as the product of (2) and (3).

The low internal efficiencies are primarily responsible for the low overall efficiencies. Possible explanations for this will be discussed in a later section.

The maximum power output of the unit was not obtained due to the limitations in volumetric capacities and maximum attainable pressures of the two air streams. Both air lines were used to capacity in run number five. The maximum pressure and volumetric flow capacity of the propane source was not approached. It is believed that higher power outputs and better

efficiencies could be obtained if better air stream sources were made available.

The combustion rate, while lower than those previously found by Mr. Sofer (6), is still considerably higher than those found in most gas turbine power plants.

Attempts to duplicate the data obtained in the first five runs failed because the meeker grid burned out. Lack of time made it impossible to take further data after a new grid had been installed.

Factors Probably Responsible for Low Internal Efficiencies

(a) Ideal cycle efficiency was computed from the approximation of the chamber pressure as measured on the secondary air line stream. Since there probably was a considerable pressure drop across the Meeker grid, the actual chamber pressure was lower than that recorded. Therefore the actual ideal cycle efficiency for each run was smaller than indicated, and consequently the ratio of internal efficiency to ideal cycle efficiency was actually greater than indicated. Although this has no effect on the absolute value of the internal efficiency, it does decrease the difference between the maximum possible thermodynamic efficiency and the actual internal efficiency. A pressure drop across the grid of three psi. will lower the ideal cycle efficiency in the higher pressure range from 27 per cent to 25 per cent and in the lower pressure range from 9 per cent to 5 per cent at those pressures.

(b) Turbulence losses due to chamber design and to the mixing of the colder secondary air with the hot fuel gases. Careful chamber design may reduce these losses.

(c) Radiation losses from the unit. These may be responsible for a considerable lowering of the internal efficiency. In the actual turbine refractory casing would probably reduce these losses.

(d) Extension of the blue flame combustion cone beyond the nozzle indicated that all of the combustion energy was not liberated inside the chamber, and hence not utilized. Operation in the higher pressure ranges shortened this cone until it was finally retained entirely within the chamber.

(e) As stated before, quenching of the flame by the secondary air results in inefficient combustion. This may be remedied by increasing the operating temperature of the chamber. However, it must be kept in mind that an increase in temperature will result in greater rejection velocities of the gases and thereby reduce the propulsion efficiency. Therefore both factors must be taken into account simultaneously and a proper balance reached.

(f) Improper nozzle design. This has been discussed in a previous section.

VI. CONCLUSIONS

It is difficult to generalize the results obtained in this thesis since a very limited amount of data was taken and optimum operating conditions were probably not reached. In addition, since efficiency and power output are affected by various factors, only conditions similar to those under which the best operating results were obtained will be discussed.

For a 6 inch diameter turbine of design similar to that in Figure 7, constructed of the titanium-base alloy, RC-130-B, with h_o/h equal to 4 and under the following conditions per chamber:

- (a) O_2 /propane weight basis 1.76
- (b) secondary air volumetric rate 9.35 cu.ft./min.
- (c) primary air volumetric rate 1.40 cu.ft./min.
- (d) chamber pressure 60 psig.
- (e) maximum wall temperature 700°F.

An internal efficiency of 8.7 per cent can be obtained, if the turbine is allowed to rotate at a peripheral velocity of 1920 ft./sec. For these conditions $\eta_p = 77.6$ per cent; $\eta_{overall} = 6.8$ per cent; and internal power output = 5.7 HP per chamber. Under these conditions no auxiliary compressor would be necessary except to initiate rotation.

It is apparent that the above turbine is neither very efficient nor produces a high power output. However, a turbine such as the above, modified so that there are six combustion chambers, three side by side along each peripheral position, would probably yield an overall efficiency of 6.8 per cent and a net power output of 34 HP.

It is apparent that the efficiencies of the Nernst type turbine will not be able to compete with those attained in ordinary gas turbines, even though higher operating temperatures are possible in the Nernst turbine. This advantage (higher operating temperatures) is partially offset by the limitations on allowable peripheral velocities. Further, in the ordinary gas turbine, compression, combustion, and expansion are carried out in three separate stages, enabling a careful control of each step to assure the optimum thermodynamic conditions. In the Nernst turbine, these three steps are carried out in the same stage and in a very small operating volume. Thus, it is necessary to compromise with the best overall operating conditions.

It is possible that the future will see the development of better heat resistant and stronger metallic alloys. However, at present, the Nernst type turbine can only compete with the gas turbine where simplicity, low costs, and small volume are important factors, but not efficiency.

VII. RECOMMENDATIONS

It is recommended that before construction of a turbine wheel is initiated, further investigations be made to determine the optimum operating conditions of a static test chamber operating at one pressure, preferably between 60 or 70 psig. These chamber pressures are compatible with the maximum allowable peripheral velocities of known heat resistant strong metallic alloys such as RC-130-B.

High pressure air compressors would be required with volumetric capacities larger than those available from the Institute high pressure line and the Nash-Hytor pump used in these investigations. The same test chamber used in these investigations could be utilized, provided that the nozzle is rebuilt to conform exactly to the chamber pressure utilized.

It is further suggested that the final design of the turbine be carefully studied in order to assure that an effective centrifugal compressor is obtained.

VIII. APPENDIX

APPENDIX A

Equation (1) on page is equivalent to:

$$x \omega = v = \sqrt{2g \frac{\sigma}{\gamma} \ln\left(\frac{h_o}{h}\right)}$$

where v is the peripheral speed at radius x . At 700°F Table I gives the maximum allowable stress, σ , as 86,000 psi. Using a safety factor of 1.2:

$$\sigma = \frac{86,000}{1.2} = 71,600 \text{ psi.}$$

$$g = 388 \text{ inches/second}^2$$

$$\gamma = 0.165 \text{ pounds/inch}^3$$

$$\frac{h_o}{h} = 3$$

$$r = 3 \text{ inches}$$

Therefore, $v = 19,330$ inches/sec. or 1610 feet/sec.

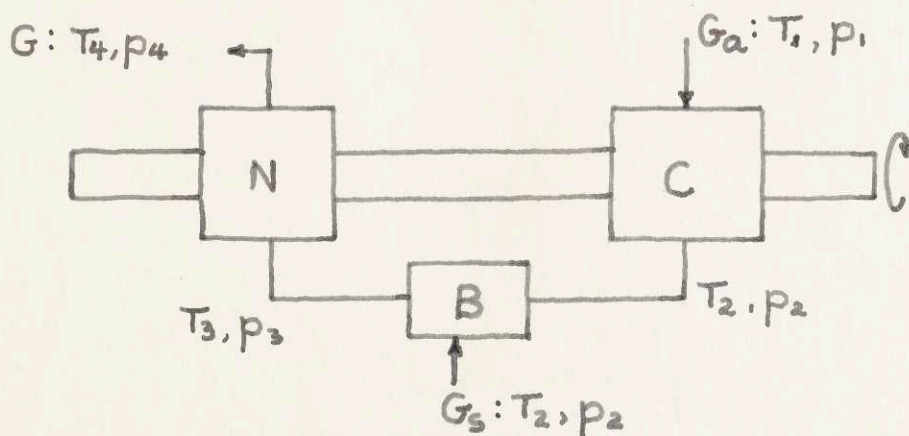
APPENDIX BFigure A

Figure A is a schematic diagram of the compression, and exhaustion cycle of the turbine under construction. Atmospheric air enters the compressor, C, and flows to the combustion chamber, B, where a stoichiometric mixture of fuel and air is injected and burned to raise the temperature of the gases. The heated gases are then exhausted through the nozzle, N, and thus expanded back to atmospheric pressure.

Thus the net available work is that excess work developed above that required to operate the compressor.

Thus:
$$W_{\text{net}} = W_{\text{nozzle}} - W_{\text{compressor}}$$

If $G_a \gg G_s$, as is the case here, $G = G_a + G_s$ also is nearly equal to G_a .

For a differential isentropic flow process:

$$dQ = TdS = dH - \frac{vdp}{J} = 0$$

$$JdH = vdp = RT \frac{dp}{p} = \frac{k}{k-1} RdT$$

and

$$\frac{dp}{p} = \frac{k}{k-1} \frac{dT}{T}$$

integration between $T = T_a$ and $T = T_b$; and $p = p_a$ and

$p = p_b$ gives:

$$\ln \left(\frac{p_b}{p_a} \right) = \frac{k}{k-1} \ln \left(\frac{T_b}{T_a} \right)$$

$$\therefore T_a = T_b \left(\frac{p_a}{p_b} \right)^{\frac{k-1}{k}}$$

The heat supplied by combustion is $c_p(T_3 - T_2)$

$$W_n = Jc_p(T_3 - T_4) \text{ and } W_c = Jc_p(T_2 - T_1)$$

Therefore the thermodynamic efficiency is:

$$\eta_T = \frac{W}{Jc_p(T_3 - T_2)} = \left(\frac{T_3 - T_4 - T_2 + T_1}{T_3 - T_2} \right)$$

$$\eta_T = 1 - \frac{T_4 - T_1}{T_3 - T_2}$$

Since both compression and expansion are isentropic:

$$T_4 = T_3 \left(\frac{p_4}{p_3} \right)^{\frac{k-1}{k}} ; \quad T_1 = T_2 \left(\frac{p_1}{p_2} \right)^{\frac{k-1}{k}}$$

and $p_1 = p_4 =$ atmospheric pressure

also $p_2 = p_3$ since combustion is at constant pressure.

$$\therefore T_4 = T_3 \left(\frac{p_4}{p_3} \right)^{\frac{k-1}{k}} = T_3 \left(\frac{p_1}{p_2} \right)^{\frac{k-1}{k}}$$

$$\text{Then } \eta_T = 1 - \frac{T_4 - T_1}{T_3 - T_2} = 1 - \frac{T_3 \left(\frac{p_1}{p_2} \right)^{\frac{k-1}{k}} - T_2 \left(\frac{p_1}{p_2} \right)^{\frac{k-1}{k}}}{T_3 - T_2}$$

$$\eta_T = 1 - \left(\frac{p_1}{p_2} \right)^{\frac{k-1}{k}} = 1 - \left(\frac{1}{r} \right)^{\frac{k-1}{k}}$$

$$\text{where } r = \frac{p_2}{p_1} = \frac{p_3}{p_4}$$

APPENDIX C

From elementary physics, the acoustic velocity for a fluid is the square root of the ratio of its bulk modulus K to its density. Thus, letting a denote the acoustic velocity,

$$a = \sqrt{\frac{K}{\rho}}$$

For an ideal gas expanding under adiabatic conditions,

$$K = k\rho$$

$$\therefore a = \sqrt{\frac{k\rho}{\rho}} = \sqrt{gk\rho V} = \sqrt{gk RT}$$

If one then defines the Mach number, M , as

$$M = \frac{v}{\sqrt{gk RT}}$$

substitution into equation (3) gives:

$$\begin{aligned} T_3 &= T_4 + \frac{v^2}{2g c_p J} = T_4 + \frac{M^2}{2g c_p J} \times k g RT_4 \\ &= T_4 \left(1 + \frac{M^2 k R}{\frac{2kR}{k-1}} \right) \end{aligned}$$

$$= T_4 \left(1 + \frac{k-1}{2} M^2 \right)$$

$$\therefore r = \frac{p_3}{p_4} = \frac{p_2}{p_1} = \left(1 + \frac{k-1}{2} M^2 \right)^{\frac{k}{k-1}}$$

APPENDIX D

If the turbine wheel is taken as a basis and its peripheral speed is v , then the kinetic energy associated with the exit gases is,

$$\text{K.E.} = \frac{(G_a + G_s)c^2}{2g} \approx \frac{Gc^2}{2g}$$

The energy consumed in bringing the air and fuel entering the turbine at zero velocity to the peripheral speed is,

$$\frac{Gv^2}{2g}$$

Thus the propulsion power is,

$$P = \frac{Gc^2}{2g} - \frac{Gv^2}{2g}$$

$$P = \frac{G}{2g} (c^2 - v^2)$$

This power is equal to the sum of the drag and frictional power, and the kinetic energy due to the absolute velocity of the exit gases,

$$P = (F_d + F_n)v + \frac{G}{2g} (c - v)^2$$

APPENDIX E

Assuming that the nozzle is one hundred percent efficient, that expansion is isentropic, and the gases have a negligible velocity in the combustion chamber, then:

$$\frac{mC^2}{2g} = Jc_p (T_3 - T_4)$$

$$T_4 = T_3 \left(\frac{1}{r}\right)^{\frac{k-1}{k}}$$

$$C^2 = \frac{2g}{m} \frac{k}{k-1} RT_3 \left[1 - \left(\frac{1}{r}\right)^{\frac{k-1}{k}}\right]$$

$$C = \sqrt{\frac{2gk}{m(k-1)} RT_3 \eta_T}$$

APPENDIX F

Derivation of propulsion efficiency equation:

$$p = \frac{v(F_d + n)}{v(F_d + n) + \frac{G}{2g} (C - v)^2}$$

From Appendix D

$$\frac{G}{2g} (C^2 - v^2) = v F_d + n + \frac{G}{2g} (C^2 - 2vC + v^2)$$

$$v F_d + n = \frac{G}{2g} (2vC - 2v^2) = \frac{G}{g} (C - v)v$$

$$\eta_p = \frac{\left| \frac{G}{g} (C-v)v \right|}{\left| \frac{G}{g} (C-v)v \right| + \frac{G}{2g} (C-v)^2} = \frac{v}{v + \frac{C}{2} - \frac{v}{2}} = \frac{2v}{v + C}$$

$$\eta_p = \frac{2 \frac{v}{C}}{1 + \frac{v}{C}} = \frac{2\theta}{1 + \theta}$$

APPENDIX H

Derivation of equation (12):

For an isentropic process,

$$\Delta h = c_p (T_3 - T_4)$$

For perfect gases, however,

$$c_p = \frac{R}{J} \left(\frac{k}{k-1} \right)$$

$$\Delta h = \frac{k}{k-1} \frac{R}{J} (T_3 - T_4)$$

$$\Delta h = \frac{k}{k-1} (p_3 v_3 - p_4 v_4) \frac{1}{J}$$

Also, since $dS = 0$

$$p_3 v_3^k = p_4 v_4^k$$

so that $v_4 = v_3 \left(\frac{p_3}{p_4} \right)^{\frac{1}{k}}$

$$\Delta H = \frac{k}{J(k-1)} p_3 v_3 \cdot \left[1 - \left(\frac{p_4}{p_3}\right) \left(\frac{p_4}{p_3}\right)^{-\frac{1}{k}} \right]$$

$$RT_3 = p_3 v_3$$

$$\Delta H = \frac{m(C_4^2 - C_3^2)}{2g}$$

$$C_4 = \sqrt{\frac{2g}{Jm} \frac{k}{k-1} RT_3 \left[1 - \left(\frac{p_4}{p_3}\right)^{\frac{k-1}{k}} \right] + C_3} \quad (12)$$

APPENDIX I

Sample Calculations

(All calculations are for Run 1)

Data taken:

Manometer reading (secondary air) = 4.7 cm.
 Downstream pressure (secondary air) = 9 psig.
 Deflection on hot part of run = 1.0 cm.

Referring to the graphs in Appendix J, $V_{\text{sec.}} = 2.0$ cu.ft./min.

$$G = \frac{29 \times 14.7 \times 144 \times 2.0}{1546 \times 530} = 0.1490 \text{ lbs. of sec. air/min.}$$

Similarly: $G_{\text{propane}} = 0.0069$ lb./min., and $G_{\text{prim.}} = 0.1095 \frac{\text{lb.}}{\text{min.}}$

$$O_2/C_3H_8 \text{ (wt.)} = \frac{\frac{0.21 \times 32 \times 14.7 \times 144 \times 1.47}{1546 \times 530}}{\frac{0.05 \times 44 \times 14.7 \times 144 \times 0.07}{1546 \times 530}} =$$

$$\frac{.21 \times 32 \times 1.47}{.65 \times 44 \times 0.07} = 4.95$$

The total mass flow was found to be:

for the hot run = 0.2654 lbs./min.
for the cold run = 0.2585 lbs./min.

whence, $G_h/G_c = 1.03$

hence the thrust = $6.25 \times \frac{1.0}{74.4} = 0.0840 \text{ lbs.} = F_h$

(where 6.25 lbs. is the weight of the unit and 74.4 cm. is the height to the pivot).

$F_c = 0.0336 \text{ lbs.}$, and corrected to hot run flow rates,

$F_c' = 0.0336 \times 1.03 = 0.0346 \text{ lbs.}$

$C_h - C_c' = \frac{(0.0840 - 0.0346) \times 60}{32.2 \times 0.2654} = 359.5 \text{ ft./sec.}$

$C_c' = \frac{3.47 \times 570 \times 1.03}{60 \times 530 \times 0.000434} = 147 \text{ ft./sec.}$ (3.47 cu.ft. is the total V_c)

$C_h = 359.5 + 147 = 507 \text{ ft./sec.}$

power output = $\frac{\text{K.E.}}{\text{sec.}} = \frac{(359^2 - 147^2) \times 0.2654}{2 \times 32.2 \times 550} = 1.75 \text{ HP}$

$$\text{Compression power required} = \frac{(147^2) \times 0.2654}{2 \times 32.2 \times 550} = 1.61 \text{ HP}$$

$$\text{hence the net available power} = 1.75 - 1.61 = 0.14 \text{ HP}$$

$$\text{Chemical energy input} = \frac{0.65 \times 44 \times 14.7 \times 144 \times 0.07 \times 19,929}{1546 \times 530 \times 60} = 17.1 \text{ BTU/sec.}$$

$$\text{or } \frac{17.1 \times 778}{550} = 24.1 \text{ HP}$$

$$\text{Internal efficiency} = \frac{0.14}{24.2} \times 100 = 0.6 \text{ o/o}$$

$$\text{Combustion rate} = \frac{0.14 \times 550 \times 3600}{778 \times 0.000503} = 0.71 \times 10^6 \text{ BTU/hr.-ft.}^3$$

$$\text{Theoretical cycle efficiency} = 100 \left[1 - \left(\frac{14.7}{23.7} \right)^{0.2855} \right] = 12.7 \text{ o/o}$$

$$M = \frac{\left(\frac{23.7}{14.7} \right)^{0.2855} - 1}{0.2} = 0.855 \quad \text{from equation (5)}$$

$$v = 1118 \times 0.855 = 956 \text{ ft./sec. (acoustic velocity} = 1118 \text{ ft./sec.)}$$

$$\eta_p = \frac{(.507 - 956)(956)}{(507 - 956)(956) + 0.5(507 - 956)^2} \times 100 = 81 \text{ o/o}$$

$$\text{Overall efficiency} = .81 \times 0.006 \times 100 = 0.5 \text{ o/o}$$

APPENDIX-J-

MANOMETER
(CM)

METER CALIBRATION
(PRIMARY AIR)

15

10

5

10

15

20

25

30

@ 1 ATM

CU. FT./MIN.

2

3

MANOMETER
(CM)

METER CALIBRATION
(FUEL)

15

10

5

10

15

20

25

30

@ 1 ATM

CU. FT./MIN.

0.1

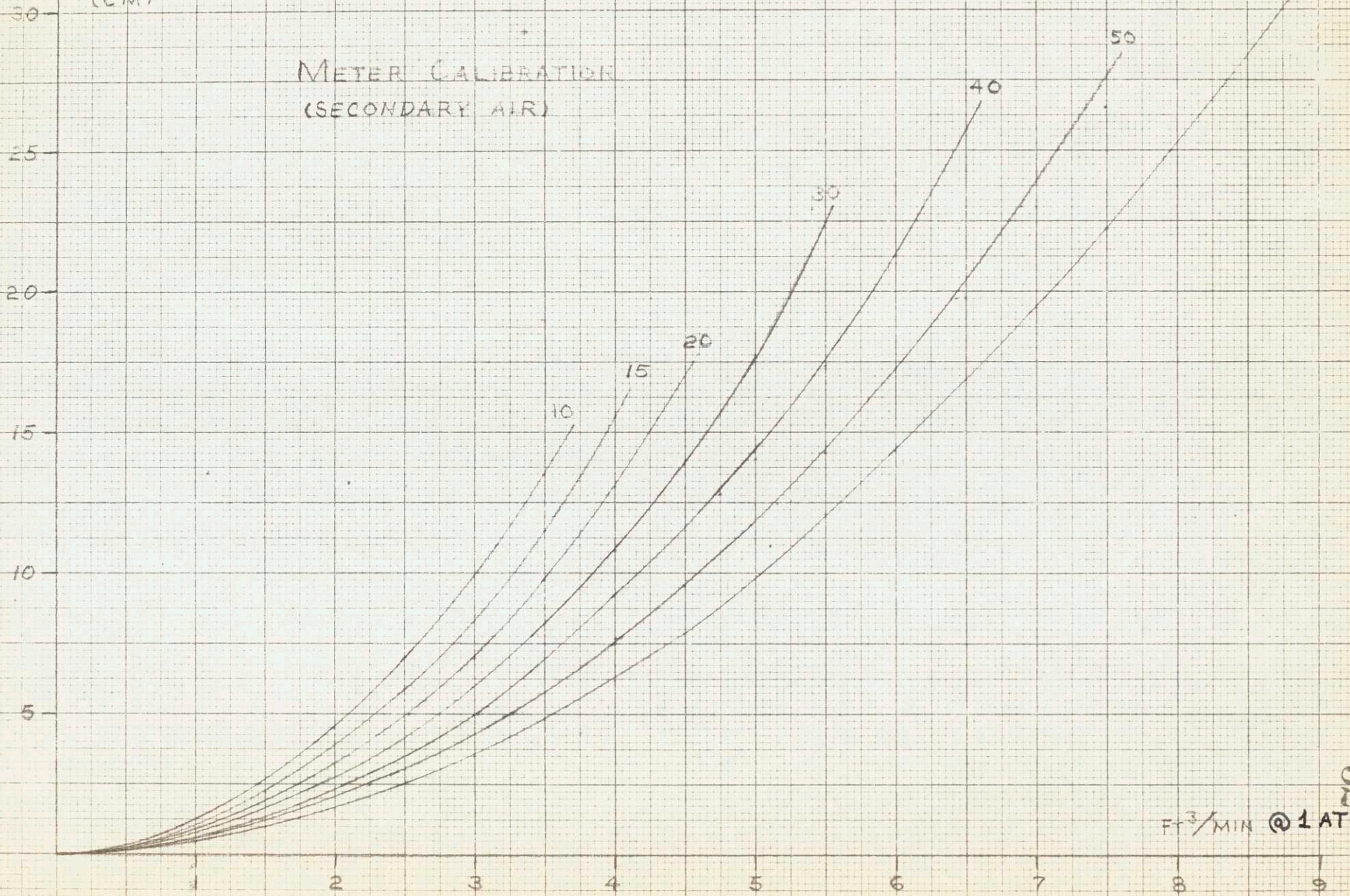
0.2

0.3

APPENDIX -J-

MANOMETER
(CM)

METER CALIBRATION
(SECONDARY AIR)



52
FT³/MIN @ 1 ATM

APPENDIX K

Data

The original data is transcribed below.

Run	Pressure		Manometer Readings			Deflection Reading*	
	Mixer	Chamber	Primary	Secondary	Fuel	Hot	Cold
1	8	9	3.9	4.7	1.6	3.2	3.8
2	7.5	14	3.9	10.1	1.2	2.8	3.4
3	9	34	2.8	20.1	1.2	1.6	2.9
4	22	50	3.3	33.0	2.8	-0.3	0.5
5 _h **	29	60	2.0	34.4	3.8	-1.3	---
5 _c	18	59	9.4	38.2	0.0	---	0.0

* The deflection is found by subtracting the deflection reading from d_0 (the reading at rest position). $d_0 = 4.2$.

** Runs 3 and 5 were the only ones for which the hot and cold run values were substantially changed. Failure to account for this change may be the reason for the disproportionate figures associated with Run 3 in Table IV.

APPENDIX LNomenclature

- a : sonic velocity, ft./sec.
 A : Area, ft.²
 c_p : Specific heat at constant pressure, Btu./lb.-°R.
 C : Velocity of jet relative to nozzle, ft./sec.
 F_d : Thrust at rim due to drag plus friction, lbs.
 g : Gravitational constant, 32.2 ft./sec.²
 h : Thickness of disc at radius x , ft.
 h' : Specific enthalpy, Btu./lb.
 h_o : Thickness of the disc at the axis, ft.
 H : Enthalpy, Btu.
 J : Mechanical equivalent of heat, 778 ft.-lbs./Btu.
 k : c_p/c_v , specific heat ratio, for air $k = 1.4$.
 K : Bulk modulus, lb./ft.²
 m : Mass, slugs.
 M : Mach number = velocity of gas / \sqrt{kgRT} , dimensionless.
 \mathcal{M} : Molecular weight, lbs./mole.
 p : Pressure, lbs./ft.²
 P : Propulsion power, ft.-lbs./sec.
 P_{n+d} : Net plus drag power, ft.-lbs./sec.
 r : Ratio of pressure in combustion chamber to that at exhaust.
 R : Gas constant, ft.-lbs./°R.-lb. = 1544/ \mathcal{M}
 R' : Gas constant = 1544 ft.-lbs./°R.-mole.

- s : Entropy/lb.
 T : Temperature, degrees rankine.
 V : Volumetric flow rate, cu.ft./min.
 v : Velocity at the rim of the turbine, ft./sec.
 \checkmark : Specific volume, ft.³/lb.
 w : Mass rate of flow at exhaust, lb./sec.
 w_s : Mass rate of flow of fuel mixture, lbs./sec.
 W : Work, ft.-lbs.
 x : Distance from axis of disc, ft.
 γ : Density of metal, lbs./ft.³
 ρ : Density of gas, lbs./ft.³
 ω : Angular velocity, radians/sec.
 θ : v/C , dimensionless.
 ϕ : Angle of deflection of test chamber support wire, degrees.
 η : Efficiency (internal), dimensionless.
 η_t : Ideal-cycle efficiency, dimensionless.
 η_p : Propulsion efficiency.
 z : $r^{1-k/k} - 1$, dimensionless.
 ψ : $\sqrt{k/k-1} \cdot \sqrt{z/1+z} \cdot (r)^{1/k}$, dimensionless.
 σ : Stress, lb./in.²

Subscripts:

- 1 : At turbine inlet.
- 2 : At combustion chamber inlet.
- 3 : At nozzle inlet.
- 4 : At nozzle outlet.
- c : Cold run data (no combustion).
- h : Hot run data (gases burning).
- a : air.
- s : stoichiometric mixture.

APPENDIX MLiterature Citations

- (1) Grant, N. F., Frederickson, A. F., and Taylor, M. E., "A Summary of Heat Resistant Alloys from 1200°F. to 1800°F., The Iron Age, March 18, April 8, April 15, 1948.
 - (2) Hottel, H. C., personal communications.
 - (3) Keenan, J. H., Kaye, J., "Calculated Heat Efficiencies for Jet Power Plants," Journ. Aeron. Science, 14, 437-450, 1947.
 - (4) Perry, J. H., Editor, "Chemical Engineering Handbook," 2nd Edition, New York, McGraw-Hill Book Co., Inc., 1941.
- Topic, Refractories:
- Alloys, Melting Points
and Mechanical Properties, page 473
- of Temperature Resisting
Alloys, page 2147
- (5) Rem-Cru Titanium, Inc., "Rem-Cru Titanium and Titanium Alloys," Midland, Pennsylvania, 1950.
 - (6) Sofer, G. A., "Nernst Type Gas Turbine," M.S. Thesis, Department of Chemical Engineering, Massachusetts Institute of Technology, Cambridge, 1949.
 - (7) Stodola, A., "Steam and Gas Turbines," Vol. II, New York, McGraw-Hill Book Co., Inc., 1927.
 - (8) Weber, H. C., "Thermodynamics for Chemical Engineers," New York, John Wiley and Sons, Inc., 1939.
 - (9) Yust, W., Editor, "Encyclopedia Britannica's 10 Eventful Years," Chicago Encyclopedia Britannica, Inc., 1947, Topic, Jet Propulsion.
 - (10) Zucrow, M. J., "Jet Propulsion and Gas Turbines," New York, John Wiley and Sons, Inc., 1947